

2013-02-25

Geochemical survey of Levante Bay, Vulcano Island (Italy), a natural laboratory for the study of ocean acidification.

Boatta, F

<http://hdl.handle.net/10026.1/1449>

10.1016/j.marpolbul.2013.01.029

Mar Pollut Bull

Elsevier BV

All content in PEARL is protected by copyright law. Author manuscripts are made available in accordance with publisher policies. Please cite only the published version using the details provided on the item record or document. In the absence of an open licence (e.g. Creative Commons), permissions for further reuse of content should be sought from the publisher or author.

Contents lists available at [SciVerse ScienceDirect](#)

Marine Pollution Bulletin

journal homepage: www.elsevier.com/locate/marpolbul

Geochemical survey of Levante Bay, Vulcano Island (Italy), a natural laboratory for the study of ocean acidification

F. Boatta^a, W. D'Alessandro^b, A.L. Gagliano^a, M. Liotta^b, M. Milazzo^a, R. Rodolfo-Metalpa^c, J.M. Hall-Spencer^c, F. Parello^{a,*}

^a DiSTeM University of Palermo, CoNISMa, via Archirafi, 36, 90123 Palermo, Italy

^b Istituto Nazionale di Geofisica e Vulcanologia, Sezione di Palermo, via U. La Malfa 153, 90146 Palermo, Italy

^c Marine Biology and Ecology Research Centre, University of Plymouth, Plymouth PL4 8AA, UK

ARTICLE INFO

Keywords:

Ocean acidification
Carbon capture and storage
Marine geochemistry
Carbonate saturation state
Volcanic vents
Carbon dioxide

ABSTRACT

Shallow submarine gas vents in Levante Bay, Vulcano Island (Italy), emit around 3.6t CO₂ per day providing a natural laboratory for the study of biogeochemical processes related to seabed CO₂ leaks and ocean acidification. The main physico-chemical parameters (*T*, pH and Eh) were measured at more than 70 stations with 40 seawater samples were collected for chemical analyses. The main gas vent area had high concentrations of dissolved hydrothermal gases, low pH and negative redox values all of which returned to normal seawater values at distances of about 400 m from the main vents. Much of the bay around the vents is corrosive to calcium carbonate; the north shore has a gradient in seawater carbonate chemistry that is well suited to studies of the effects of long-term increases in CO₂ levels. This shoreline lacks toxic compounds (such as H₂S) and has a gradient in carbonate saturation states.

© 2013 Elsevier Ltd. All rights reserved.

1. Introduction

Over 265×10^9 metric tonnes of C (mainly as CO₂) have been released to the atmosphere since 1750 (United Nations, 2001) with half of those emissions having occurred since the mid-1970s. About one third of the anthropogenic CO₂ released into the atmosphere in the past two centuries has been taken up by the ocean (Sabine et al., 2004) and the current annual rate of global oceanic uptake is estimated to be 2.2×10^9 metric tonnes C (Mikaloff-Fletcher et al., 2006). In aquatic systems CO₂ gas dissolves, hydrates and dissociates to form weak carbonic acid, which is the main driver of natural weathering reactions (Drever, 1997). As the ocean surface absorbs CO₂, pH is lowered according to the following reaction:



Increasing atmospheric CO₂ acidifies surface seawater; surface seawater pH has already decreased globally by 0.1 units (called *ocean acidification*, OA), which corresponds to a 30% increase in the concentration of H⁺ ions (Sabine et al., 2004). Projected global CO₂ emissions are expected to further lower ocean pH by 0.1–0.35 units this century (Solomon et al., 2007). Our understanding of how increasing ocean acidity can affect marine ecosystems is mostly gathered using *in vitro* experiments (e.g. Riebesell et al.,

2007). Hall-Spencer et al. (2008) proposed augmenting this approach by using environments that have naturally high levels of pCO₂ such as around volcanic vents.

Several submersed CO₂ vent systems are present in deep (>100 m); nearshore (<100 m), and shallow water (<5 m) sites in the Aeolian archipelago (north-eastern Sicily, Italy) (Italiano, 2009). The Aeolian archipelago, consisting of eight volcanic islands and numerous seamounts, is regarded as a typical volcanic arc generated by subduction processes in the Southern Tyrrhenian sea-floor (Barberi et al., 1974; Beccaluva et al., 1985). There are two active aerial volcanoes on the islands of Stromboli and Vulcano, while volcanic activity of steaming fumaroles and submerged seeps are found on most of the islands. The southernmost volcanic island of Vulcano has several minor volcanic centres (Keller, 1980) with intense submersed CO₂-dominated seeps at Levante Bay. Aerial and submarine gas analyses have shown that these underwater seeps originate from a different eruptive fracture system than that of the recent Fossa cone eruption, likely related to the Vulcanello crater eruption in the 16th century (Tedesco et al., 1995).

The aims of the present study were twofold: (1) to characterise most prominent geochemical parameters of the waters of Levante Bay (Fig. 1) and (2) to provide a thorough assessment on the spatio-temporal variability of pH/CO₂ along the northern shore of the bay where ocean acidification studies have begun. The northern shore is situated well away from the main vents but has acidified waters that form a shallow pCO₂ gradient along ca. 200 m of rocky and sandy habitats (Johnson et al., 2013; Arnold

* Corresponding author. Tel.: +39 09123861643.

E-mail address: francesco.parello@unipa.it (F. Parello).

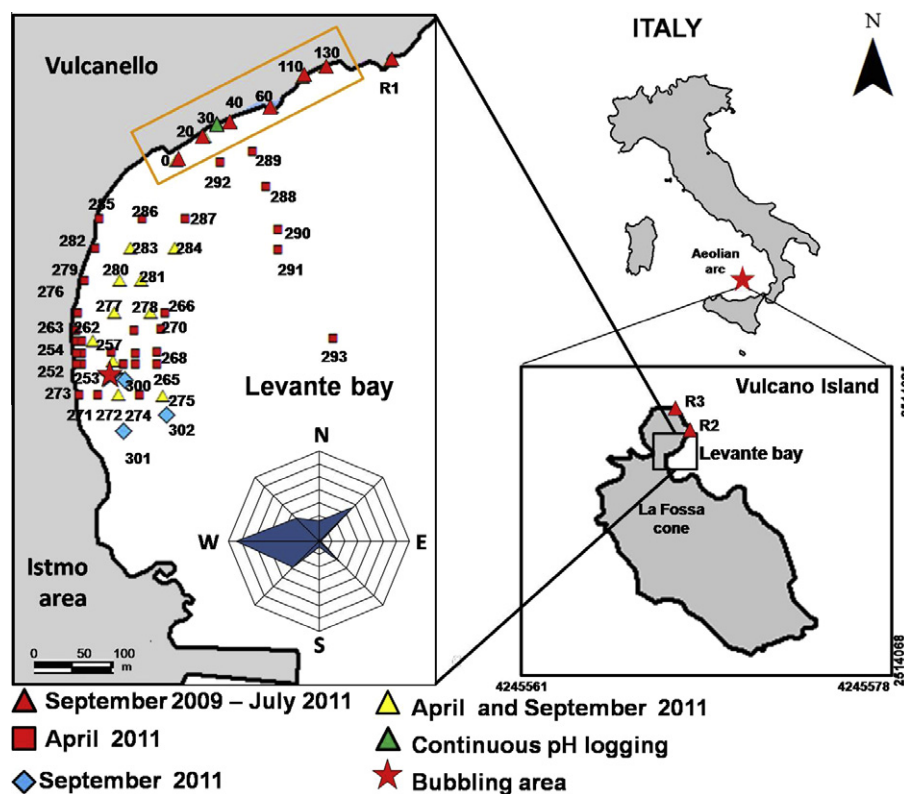


Fig. 1. Location of the study area and distribution of the sampling sites.

et al., 2012; Lidbury et al., 2012). Such baseline chemical studies are essential if we are to understand biological responses to volcanic vents and how they apply to ocean acidification (Kerrison et al., 2011). Our results show that much of the bay around the vents was corrosive to calcium carbonate and that shallow waters at >300 m from the main leaks had a gradient from normal sea water pH_T (8.1–8.2) to lowered pH_T (mean 7.8–7.9, minimum 7.4–7.5) that is well suited to studies of CO_2 seabed leakage and chronic ocean acidification.

2. Materials and methods

2.1. Site description

Volcanic activity on Vulcano island started in the upper Pliocene (Frazzetta et al., 1984) with the first subaerial activity dated at 120 ka building up a trachybasaltic – trachyandesitic stratocone in the south of the island (Keller, 1980). During the last 10 ka volcanic activity has produced a cone called La Fossa Crater at 391 m above sea level; it last erupted in 1888 and 1890 (Silvestri and Mercalli, 1891). Levante Bay on the northeastern side of Vulcano island (Fig. 1) has gas vents along an active fault (Frazzetta et al., 1984). The main underwater venting gas field occur at less than 1 m depth on the southwestern part of Levante Bay ($38^{\circ}25'01''N$, $14^{\circ}57'36''E$), and extends over a 130×35 m area adjacent to a sandy beach in the Istmo area (Fig. 1). Inguaggiato et al. (2012) estimated the total bubbling CO_2 output of the bay is about 3.6 tonne/day. Tidal range is minimal (<40 cm) and currents are mostly wind-driven. Predominant winds belong to western north-western sectors, therefore acidified water masses mostly run parallel to the northern shoreline of the bay (Fig. 1).

After the last eruption on Vulcano some authors reported wide fluctuations in the hydrothermal activity and consequent changes in the gas composition (Sicardi, 1940). In 1938, Sicardi reported

H_2S concentrations in the gas emissions on the sea shore between 8.4 and 4.7 vol.%. A shallow geothermal aquifer was found during exploratory drilling between 1951 and 1957 in the Levante Bay area (Sommaruga, 1984). Gas emissions from the geothermal aquifer are thought to result from magmatic and hydrothermal fluid mixing, feeding the crater fumaroles and then cooling (Chiodini et al., 1993, 1995). Capaccioni et al. (2001) found that the underwater gas emissions of Levante Bay were 97–98% CO_2 with 2.2% H_2S close to the vents falling to less than 0.005% H_2S on the north-western part of the beach of Levante Bay (Table 1 and Fig. 1). These authors attributed the variability in Levante Bay gas discharge to variable interactions between iron sulphides and weakly acid waters (Capaccioni et al., 2001). More recently, in the same bubbling area Carapezza et al. (2011) quantified the CO_2 and H_2S fluxes, showing the most intense degassing area bubbles ca. 1 tonne/day of CO_2 and ca. 15 kg/day of H_2S .

2.2. Sampling and analytical methods

A grid of sampling points was used to map the seawater chemistry of Levante Bay in April and September 2011. Most of the samples were positioned around the underwater vents and along the beach of the Istmo area. Additional sampling points parallel to the northern shore were located away from the venting gas field, where pH values were comparable to those expected due to carbon dioxide emissions this century (Caldeira and Wickett, 2003) (Fig. 1).

During April 2011, 40 water samples were collected and analysed for the presence of dissolved gases as well as major and minor elements. These samples were also used to determine the influence of heated water emissions. Water samples for chemical analyses were collected and stored in prewashed HDPE bottles. Major element analyses were carried out on unfiltered (Cl and SO_4) and filtered and acidified (Na, K, Ca and Mg) samples by ion

Table 1

Chemical composition of the gases in Levante Bay area.

Site	Date	CO ₂ (%)	N ₂ (%)	O ₂ (%)	CH ₄ (ppm)	H ₂ (ppm)	H ₂ S (ppm)	References
Isthmus	1989	96.0	3.3	0.2	460	1300	18,000	Italiano et al. (1984)
Sea shore	1990	98.5	1.6	<0.05	1025	17	9000	Italiano et al. (1984)
FM	May 1995	96.7	0.6	0.0001	760	4600	21,600	Capaccioni et al. (2001)
Vu1	May 1996	98.1	1.0	0.0001	1020	7.2	8000	Capaccioni et al. (2001)
Vu2	May 1997	97.8	1.0	0.0001	710	774	10,200	Capaccioni et al. (2001)
Vu3	May 1998	76.2	23.2	0.0001	1710	10.8	50	Capaccioni et al. (2001)
FM	November 1995	97.7	0.8	0.0002	550	6600	15,100	Capaccioni et al. (2001)
Vu1	November 1996	98.2	1.0	0.22	1440	5.6	6100	Capaccioni et al. (2001)
Vu2	November 1997	97.8	1.0	0.06	960	568	10,500	Capaccioni et al. (2001)
Vu3	November 1998	84.6	15.2	1.8	1710	5.4	<50	Capaccioni et al. (2001)
Grip	2001	98.6	1.4	n.r.	1500	2374	n.r.	Amend et al. (2003)
Acque Calde 2	2001	98.8	0.9	n.r.	1290	19,800	n.r.	Amend et al. (2003)
Campo Frizzante I	2003	99.1	0.8	n.r.	1320	570	n.r.	Rogers et al. (2007)
Campo Frizzante II	2003	99.0	0.9	n.r.	1360	<5	n.r.	Rogers et al. (2007)
I-1	2010	98.6	0.9	0.08	1400	1410	n.r.	Inguaggiato et al. (2012)
I-5	2010	97.6	0.8	0.07	1300	1390	n.r.	Inguaggiato et al. (2012)
I-15	2010	96.9	1.2	0.16	1400	1520	n.r.	Inguaggiato et al. (2012)
I-26	2010	97.5	1.1	0.13	1300	1380	n.r.	Inguaggiato et al. (2012)
I-37	2010	98.3	1.0	0.12	1400	1450	n.r.	Inguaggiato et al. (2012)
Vent (free gas)	April 2011	98.0	1.5	0.21	1700	<5	400	This study
Vent (dissolved gas)	April 2011	13.0	64.5	0.17	430	<5	n.a.	This study

n.r. = not reported; n.a. = not analysed.

chromatography and alkalinity by titration with 0.1 N HCl. Samples for trace elements analysis were filtered in the field through 0.45 µm Millipore MF filters and then acidified to pH ≈ 2 with ultrapure HNO₃ and analysed for B, Sr and Fe by ICP-MS. Accuracy and precision of these measurements were computed by analysing certified reference materials and performing replicates on samples. A gas sample was collected at the most actively bubbling site with an inverted funnel and a glass sampler with two gas-tight stopcocks. Dissolved gases were collected and analysed utilising the procedure described in Liotta and Martelli (2012). This method is based on the equilibrium partition of gases between a liquid and a gaseous phase after the introduction of host gas (Ar). Gas concentrations were measured using the GC Perkin–Elmer Clarus 500 equipped with Carboxen 1000 columns, Hot Wire and Flame Ionisation detectors with methanizer and Ar as carrier gas. The gas samples were injected through an automated injection valve with a 1000 µL loop. Calibration was made with certified gas mixtures. Analytical precision ($\pm 1\sigma$) was always better than $\pm 5\%$. Standard chemical analyses (major, minor, trace elements and dissolved gases) were all made on subsamples of the same water sample allowing comparability of the results. Dissolved H₂S (S⁻) measurements were carried out using Draeger tubes (range 2–300 ppm, detection limit 0.5 ppm).

In April and September 2011, the main physico-chemical parameters (temperature, pH, Eh and electrical conductivity) were measured using a 556 MPS YSI (Yellow Springs, USA) probe at 70 sites (Fig. 1). Temperature, pH and Eh measurements were within ± 0.1 °C; ± 0.05 pH_T units, and ± 1 mV respectively, while conductivity data were $\pm 2\%$. The pH-meter was calibrated using TRIS/HCl and 2-aminopyridine/HCl buffer solutions (DOE, 1994). As for other volcanic vents systems (Fabricius et al., 2011; Kerrison et al., 2011) we recorded pH fluctuations along the shallow CO₂ gradient in the northern shore of the bay (triangles in Fig. 1), with measurements were repeated on several visits from September 2009 to July 2011 under different weather conditions and at various hours of the day. For each site along the north shore, average pH values were calculated from hydrogen ion concentrations before re-converting back to pH values, using the collected dataset. To assess pH variability, we used an *in situ* modified Honeywell Durafet pH sensor to record pH and temperature hourly. The sensor was deployed at 1 m depth at site 30 (where our monitoring data had an average pH_T of 7.7 units) from April 26th to May 30th, 2010.

The sensor was removed for 1.5 days to avoid damage during a storm. Discrete water samples were collected for Total Alkalinity (TA) within 0.25 m of the pH sensor during the initial deployment and the retrieval of the sensor. Additional water samples for TA analyses were collected at each site along the north shore from September 2009 to July 2011. One hundred ml of water sample was passed through 0.2 µm pore size filters, poisoned with 0.05 ml of 50% saturated mercuric chloride (HgCl₂) to stop biological activity, and then stored in the dark at 4 °C. Three replicate sub-samples were analysed at 25 °C using a titration system. The pH was measured at 0.02 ml increments of 0.1 N HCl. Total alkalinity was calculated from the Gran function applied to pH variations from 4.2 to 3.0, as $\mu\text{mol kg}^{-1}$ from the slope of the curve HCl volume versus pH. Titrations of TA standards provided by A.G. Dickson (batch 99 and 102) were within 0.6 $\mu\text{mol kg}^{-1}$ of the nominal value. Parameters of the carbonate system (pCO₂, CO₃²⁻, HCO₃) and saturation state of calcite and aragonite were also calculated from pH_T, TA, temperature and salinity using the free-access CO₂ SYStat package (Pierrot et al., 2006). Dissociation constants of H₂CO₃ and HCO₃⁻ were derived from Roy et al. (1993). Data are reported as mean and standard deviation throughout the manuscript.

3. Results

3.1. Geochemistry of Levante Bay

3.1.1. Physico-chemical parameters and saturation indexes

Both Eh and pH_T were greatly affected by the main vent gas emissions. Eh values ranged from –152 to 170 mV in April 2011 and from –23 to 171 mV in September 2011 (Table 2), while pH_T values range between 5.70 and 8.05 in April and from 6.05 to 8.03 in September (Table 2). As expected, the lowest values of Eh and pH were recorded within the main vent area, both in April and September 2011 (Fig. 2a–d). Electrical conductivity did not show great variations in April 2011, being generally close to the mean value of 46.8 mS/cm (Table 2). Seawater temperatures ranged on average between 16.0 and 18.6 °C in April 2011 and between 25.3 and 26.9 °C in September 2011 (Table 2). Warmer waters were recorded near the bubbling area, whilst in the northern part of the Levante Bay waters were cooler (see also Fig. 2e). In April 2011, Total Alkalinity in the area around the vent ranged from

Table 2
Summary of physico-chemical and chemical analyses on water samples of Levante Bay in April ($n = 70$) and in September ($n = 21$) 2011.

		Min	Max	Average	SD	Ambient seawater
<i>April</i>						
Eh	mV	−157	162	−53	93	
pH		5.64	8.05	7.11	0.69	
Electrical conductivity	mS/cm ³	45.4	49.7	46.8	0.7	
Temperature	°C	16.0	18.6	17.2	0.5	
Total alkalinity	mmol/kg	2.78	3.17	2.92	0.10	
Ω_{CALC}		0.03	5.63	1.76	1.89	
Ω_{ARAG}		0.02	3.64	1.14	1.22	
Cl [−]	mmol/kg	521	590	574	14	558 ^a
SO ₄ ^{2−}	mmol/kg	26.9	30.3	29.4	0.6	28.9 ^a
Na ⁺	mmol/kg	464	501	487	7.2	479 ^a
K ⁺	mmol/kg	10.3	12.2	10.8	0.4	10.4 ^a
Mg ²⁺	mmol/kg	53.8	58.5	56.2	0.9	54.3 ^a
Ca ²⁺	mmol/kg	10.4	12.7	10.9	0.4	10.5 ^a
B	μmol/kg	380	553	447	39	421.5 ^b
Fe	μmol/kg	0.057	8.10	1.62	1.90	0.062 ^b
Sr	μmol/kg	88	134	102	10	94.7 ^b
H ₂	mL/L (STP)	0.0008	0.128	0.018	0.031	7.46 × 10 ^{−6c}
O ₂	mL/L (STP)	0.04	4.95	3.11	1.21	5.11 ^c
N ₂	mL/L (STP)	5.20	11.24	9.49	1.54	9.52 ^c
CH ₄	mL/L (STP)	0.0001	0.0122	0.0023	0.0033	5.36 × 10 ^{−5c}
CO ₂	mL/L (STP)	0.31	103	12.6	22.9	0.28 ^c
<i>September</i>						
Eh	mV	−23	171	111	52	
pH		6.05	8.03	7.03	0.68	
Temperature	°C	25.3	26.9	26.0	0.4	
Total alkalinity	mmol/kg	2.52	3.21	2.88	0.16	
Ω_{CALC}		0.06	5.42	1.59	1.89	
Ω_{ARAG}		0.12	4.64	1.42	1.51	

^a Average concentrations of major elements at 25 °C and 35‰ salinity (Sources: Wilson, 1975; Millero and Schreiber, 1982).

^b Source: Turekian, 1968.

^c ASSW (theoretical Air-Saturated SeaWater at 20 °C and 37‰ salinity).

2.78 to 3.17 μmol kg^{−1} (Table 2). Ω_{CALC} and Ω_{ARAG} ranges were 0.03–5.63 (mean 1.76 ± 1.89; $n = 70$) and 0.02–3.64 (mean 1.14 ± 1.22; $n = 70$) (Table 2), respectively. Therefore, most of the sampling sites were under-saturated with respect to aragonite (Fig. 2f). Saturation in the Levante Bay is achieved only in the northern part where pH values exceed either 7.5 for calcite (not shown) or 7.6 for aragonite (Fig. 2f).

3.1.2. Chemical composition of the waters

Major elements (Cl, SO₄, Na, K, Ca and Mg) generally had very low variability across the Levante Bay, with average values very close to the Mediterranean Sea surface waters and a standard deviation within the precision of the method (±3%) (Table 2). Boron and Strontium concentrations had a slightly higher variability from 380 to 553 μmol kg^{−1} and from 88 to 134 μmol kg^{−1} (Table 2). On the other hand iron concentration ranged from 0.06 to 8.1 μmol kg^{−1}, being up to two orders of magnitude higher than that normally found in the Mediterranean Sea (Table 2). The distribution map of dissolved iron shows that the maximum values were recorded along the shore close to vents area, indicating a limited input correlated to hydrothermal fluids in liquid phase (Fig. 3). Dissolved sulphide was <55 μmol kg^{−1} in the main vent area of Levante bay and below the detection limit (i.e., <15 μmol kg^{−1}) already at 5 m distance from the degassing area.

3.1.3. Gas composition

The composition of the free gas sample collected in April 2011, at the most vigorous bubbling site is given in Table 1, for comparisons with the gas compositions of the same area taken from the literature and referring to the period 1989–2011. All gases are mainly composed of CO₂ with concentrations generally above 95% by volume (Table 1). The main atmospheric gases (N₂ and O₂) are generally limited to few % with N₂ always in excess with

respect to the N₂/O₂ ratio of the atmosphere. Typical hydrothermal gases (H₂, CH₄ and H₂S) had concentrations ranging from few ppm to few %. Methane had the lowest variability (430–1710 ppm) with the April 2011 samples falling at the higher end of the range. The highly reactive species (H₂ and H₂S) had a greater variability and the April 2011 samples had values at the lowest end of the range we detected (Table 1).

Dissolved gases (expressed as mL/L (STP)) are given in Table 3 for most of the collected samples. All the samples fall between two end members (Fig. 4a): the air saturated seawater (hereafter ASSW) and CO₂ rich water. A clear alignment can be recognised thus suggesting that atmospheric contribution to dissolved gases always play an important role. However, if we look at N₂/O₂ ratio, many samples exhibit higher values with respect to the ASSW, probably due to the oxygen consumption occurring in reducing environments. Most of the samples are also enriched with respect to ASSW in methane and hydrogen (Table 3). The ternary diagram of CH₄–N₂–CO₂ confirms the atmospheric contribution to dissolved gases and shows variable ratios between CH₄ and CO₂ (Fig. 4b). Highest levels of dissolved CO₂ and CH₄ and lowest levels of dissolved O₂ were recorded close to the main hydrothermal vents, whilst the opposite (i.e. close to ASSW concentrations) were recorded along the northern part of the bay (Table 2 and Fig. 5a–c).

3.2. A geochemical focus on the northern shore of the Levante Bay

An extensive carbonate chemistry gradient is caused by the CO₂ vents of the southern part of the Levante Bay. A pH gradient runs parallel to the north-eastern coast of the island along the Vulcanello shoreline (Fig. 6a–d). Along the northern shore of the bay, from September 2009 to July 2011 the pH ranged on average from 7.49 ± 0.29 to 8.19 ± 0.04, whilst pCO₂ ranged from 3361.7 ± 2971.3 μatm to 424.6 ± 61.5 μatm. The ambient seawater

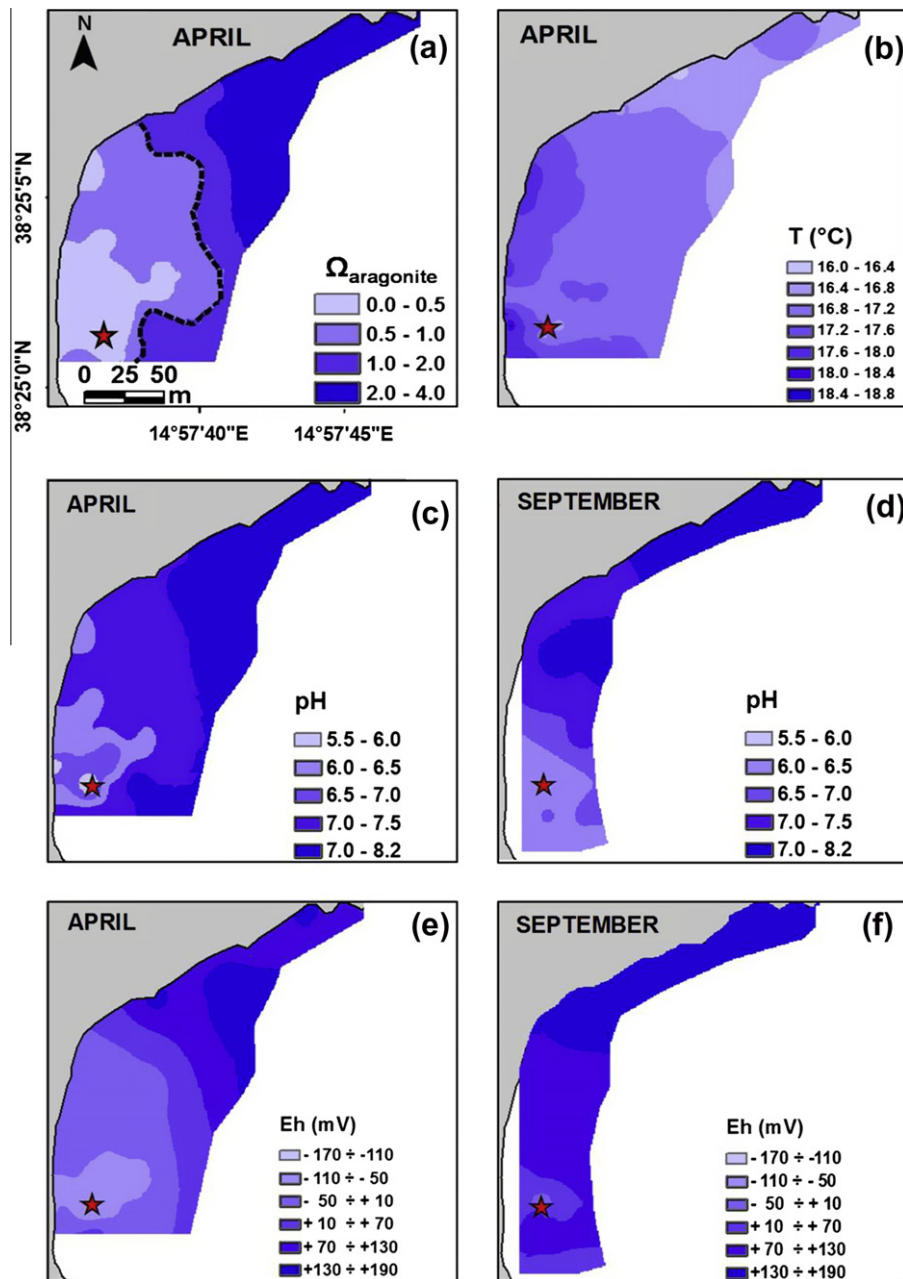


Fig. 2. (a) Distribution map of the Ω_A measured in the waters of the Levante Bay in April 2011. Values are calculated from the physico-chemical parameters. The dashed line represents the limit between oversaturated and undersaturated waters. (b) Distribution map of the seawater temperature measured in the Levante Bay in April 2011. (c and d) Distribution maps of the seawater pH values measured in the Levante Bay in April and in September 2011, respectively. (e and f) Distribution maps of the seawater Eh values measured in the Levante Bay in April and in September 2011, respectively. The red star represents the position of the gas vent area. (For interpretation of the references to colour in this figure legend, the reader is referred to the web version of this article.)

pH/pCO₂ level were reached at ca. 400 m from the intense CO₂ leakage site around the sites 110 and 130 (Fig. 6a and c). More specifically, three distinct carbonate chemistry zones associated with vent activity were found, with reduced mean pH and increased temporal variability at sites closer to the vent area (Fig. 6a): (1) a very low pH zone at 0–20 sites (7.56 ± 0.37 and 7.49 ± 0.29 pH_T, respectively); (2) a low pH zone at 40–60 sites (7.84 ± 0.24 and 7.94 ± 0.24 pH_T); (3) and a normal pH zone at 110–130 sites (8.05 ± 0.21 and 8.12 ± 0.14 pH_T). pH at reference sites (R1–R3) ranged on average from 8.14 ± 0.04 to 8.19 ± 0.09 pH_T. Although the variability in pH was similar among low and very low pH zones, the variability in other carbonate parameters was much

higher in the very low pH zones reflecting the logarithmic scale of pH (Fig. 6a–d). Ω_{CALC} ranged on average from 1.76 ± 1.36 to 6.28 ± 0.79 (Fig. 6b), whilst Ω_{ARAG} values ranged from 1.16 ± 0.91 to 4.14 ± 0.57 (Fig. 6d). Interestingly, we also recorded relatively constant total alkalinities (on average 2517.1 – 2541.3 $\mu\text{mol kg}^{-1}$ (6), temperatures (21.53 – 23.96 °C), and salinities (37.18 – 37.63 ‰) across the northern shore and reference shallow sites (Table 4).

Continuous monitoring of seawater pH at site 30 on the northern shore revealed the short-term temporal variability of the shallow waters pH. During the whole period pH_T values ranged from 6.62 to 8.06 units and an average value of 7.65 ± 0.26 was recorded ($n = 807$) (Fig. 7). More specifically, two thirds of the hourly pH

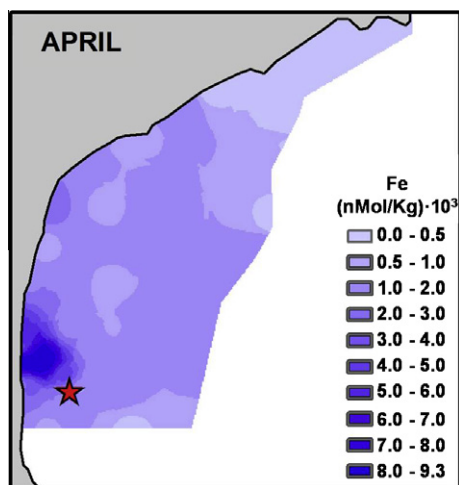


Fig. 3. Distribution map of the seawater iron concentrations measured in the Levante Bay in April 2011.

measurements were below 7.8 pH_T units, 30.2% were between 7.8 and 8.0 and 2.2% above 8.0.

4. Discussion

About 3.6 tonnes of CO₂ bubble into Levant Bay per day (Inguaggiato et al., 2012) which strongly influences the seawater chemistry of the bay. The pH formed a clear gradient from 5.65 at the main gas vents increasing to 8.1 (which is typical for Mediterranean seawater), in the north-eastern part of the bay. Elevated seawater temperatures were found close to the vents due to heating by geothermal steam (Aiuppa et al., 2000). Moving away from

the gas vents towards the northern part of the bay, N₂ and O₂ returned to normal values due to water-atmosphere exchange yet CO₂ remained elevated. Accordingly, dissolution of these gases produces the observed enrichment in CO₂ and in a lesser extent in CH₄. In the ternary diagram CH₄–N₂–CO₂, the variability of CH₄/CO₂ ratio could result from the preferential CO₂ dissolution and consequent conversion to carbonate and bicarbonate species.

The dissolved gases do not reach equilibrium with the bubbling gases. The most CO₂-enriched dissolved gas sample was collected at the same site where the free-gas sample has been taken. Comparing the dissolved and the free-gas composition (Table 1), the former has a much lower content in CO₂ and a higher N₂ content with respect to the latter, confirming that equilibrium was not reached due to the short interaction time.

The April 2011 Eh map shows a large area with negative values; this month had light winds, calm seas and restricted water exchange between the bay and the open sea. September 2011 was windier, with more water exchange, and negative Eh values only occurred very close to the main gas vents. Dissolved CO₂ and CH₄ were highest close to the vents and decreased to background levels in the north-eastern part of the bay. The vent area had the lowest dissolved oxygen levels which, together with the lowest Eh values, reflect oxygen consumption due to the oxidation of metals such as iron and reduced gases like H₂ and H₂S. Iron concentrations from the underwater CO₂ seeps in Levante Bay are about an order of magnitude higher than reported for other near-shore oligotrophic Mediterranean waters (Kadar et al., 2012), strongly indicating that this type of cold shallow CO₂ seeps can supply significant iron input to the sea. Such iron-rich (up to 2 mol kg⁻¹) shallow hydrothermal groundwaters in the Istmo area were also recorded by Aiuppa et al. (2000). Alternatively, the high iron concentrations recorded in this area may also derive from an increased leaching from the sediments due to the extreme low pH levels, as recently suggested by Roberts et al. (2013).

Table 3

Chemical analyses of the dissolved gases in the waters of Levante Bay, including the northern shore (0–130) and the reference (R1) sites (in bold).

Sample	Date	H ₂ mL/L (STP)	O ₂ mL/L (STP)	N ₂ mL/L (STP)	CH ₄ mL/L (STP)	CO ₂ mL/L (STP)
Vent	4-04-2011	n.d.	0.044	8.03	0.01215	103.2
252	4-04-2011	0.0789	3.50	10.86	0.00165	8.77
253	4-04-2011	0.0064	3.31	10.29	0.00482	31.04
254	4-04-2011	0.0033	2.29	9.95	0.00491	40.15
256	4-04-2011	0.0411	1.80	9.66	0.00606	17.51
257	4-04-2011	0.0045	4.25	10.51	0.00123	0.87
258	4-04-2011	0.0266	1.94	10.08	0.01216	56.91
259	4-04-2011	0.0212	3.10	10.44	0.00299	24.06
262	4-04-2011	0.1283	2.66	10.61	0.00276	23.68
264	5-04-2011	0.0276	3.88	10.86	0.00111	2.01
265	5-04-2011	0.0017	3.59	11.24	0.00110	1.12
266	5-04-2011	n.d.	3.64	9.62	0.00105	3.95
267	5-04-2011	n.d.	2.56	9.41	0.00389	24.51
269	5-04-2011	n.d.	2.82	8.53	0.00189	2.19
281	5-04-2011	n.d.	3.87	10.35	0.00108	1.13
283	5-04-2011	0.0056	4.43	9.65	0.00080	2.56
288	6-04-2011	0.0069	2.11	6.41	0.00031	0.31
289	6-04-2011	0.0051	4.87	10.85	0.00019	0.44
290	6-04-2011	0.0011	2.52	5.20	0.00012	0.49
291	6-04-2011	0.0052	0.51	10.70	0.00015	1.13
292	6-04-2011	0.0062	3.33	10.40	0.00022	0.87
0	6-04-2011	0.0008	3.33	9.58	0.00016	2.33
20	6-04-2011	0.0015	2.97	8.50	0.00047	2.00
40	6-04-2011	0.0171	2.10	5.63	0.00023	0.66
60	6-04-2011	0.0023	4.44	8.88	n.d.	0.42
110	6-04-2011	0.0035	3.54	9.68	0.00038	0.44
130	6-04-2011	n.d.	4.82	10.08	0.00034	0.36
R1	6-04-2011	0.0027	4.95	9.76	0.00013	0.34
ASWW		7.46 × 10 ⁻⁶	5.11	9.52	5.36 × 10 ⁻⁵	0.28

Sample identification as in Fig. 1; n.d. = not detected. ASWW is the theoretical Air-Saturated Sea Water at 20 °C and 37.0 salinity.

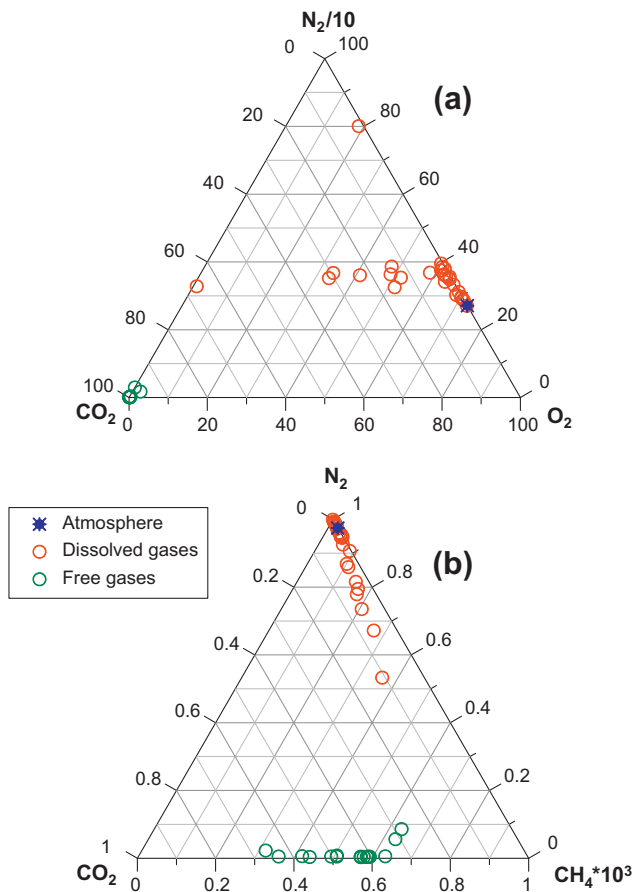


Fig. 4. (a) CO_2 - N_2 - O_2 and (b) CO_2 - N_2 - CH_4 triangular plots showing the composition of the dissolved (in red) and bubbling (in green) gases of the Levante Bay. Dissolved gases have been recalculated as theoretical partial pressure value in order to be comparable to the free gas phase of the bubbling gases. (For interpretation of the references to colour in this figure legend, the reader is referred to the web version of this article.)

Hydrogen sulphide is a low temperature product of hydrothermal activity. The high temperature emissions of the La Fossa Crater contain acidic gases like SO_2 , HCl and HF that upon dissolution in the hydrothermal system cause very low pH values (Aiuppa et al., 2000). Iron sulphides, mainly marcasite and pyrrhotite, coat rocks or occur as grains on Vulcano due to the effect of acid waters on sulphides according to the reaction $\text{FeS} + 2\text{H}^+ = \text{Fe}^{2+} + \text{H}_2\text{S}$.

Sedwick and Stüben (1996) measured H_2S concentrations of 273 and $166 \mu\text{mol kg}^{-1}$ at the most intense bubbling sites while

Amend et al. (2003) found values from 20 to $320 \mu\text{mol kg}^{-1}$ in the bay area. In April 2011, we found $<55 \mu\text{mol kg}^{-1}$ in the bubbling area. Our Eh and pH data show that almost all samples fall in the stability field of sulphate and very few, close to the bubbling site, in that of hydrogen sulphide. Such data together with the low sulphide (S^{2-}) concentrations we recorded in the water at 5 m distances from the main vent area ($<15 \mu\text{mol kg}^{-1}$), suggest that due to the oxidation to non-toxic sulphate in the O_2 -rich environment of the bay, only a small proportion of the H_2S brought by the hydrothermal fluids enters or remains into the aquatic phase. Considering for sulphide a similar decay with the distance from the vents, as for dissolved CO_2 , we consider that the northern transect is not influenced by hydrogen sulphide. The positive Eh values measured in the area of the northern transect corroborate this assumption.

4.1. The northern shore of Levante Bay

Our monitoring from September 2009 to September 2011 at shallow sites along the northern shore of Levante Bay allowed us to differentiate three carbonate chemistry zones influenced by the vent activity, and extending along ca. 200 m of coast. Specifically, at sites >300 m from the intense CO_2 leakage site, we recorded reduced mean pH ($<7.6 \text{ pH}_T$ units), and increased temporal pH variability, whereas ambient seawater pH/ pCO_2 conditions were found at ca >400 m. pH was highly variable in the low pH zone (site 30), as showed during the 1 month hourly measurements. The lowest pH_T was 6.62 and averaged $7.65 (\pm 0.26)$, with two thirds of the measurements below 7.8 pH_T units, that is the projected average global sea surface pH value for the year 2100 (Caldeira and Wickett, 2003). At this value most subtidal calcifiers may disappear in oligotrophic parts of the Mediterranean (Hall-Spencer et al., 2008). Daily and seasonal variations in seawater pH from 7.5 to 9.0 have been reported in coastal habitats (Middelboe and Hansen, 2007) and a compilation of high resolution time series of upper ocean pH has highlighted wide and rapid natural fluctuations in many coastal ecosystems, including vents (Hofmann et al., 2011). This natural variability was seldom considered in the early stages of ocean acidification research as perturbation experiments mainly investigated the responses of organisms to constant low pH. It may prove useful to incorporate natural pH variability in ocean acidification studies as ambient fluctuations in pH may have a large impact on marine organisms, affecting their performance (Hofmann et al., 2011). Importantly, dissolved hydrogen sulphide from the seeps, potentially toxic for cellular respiration, does not extend to the northern shore as previously stated. At these distances sulphide (S^{2-}) was absent and sulphate (SO_4^-) levels were typical for oceanic waters, suggesting that only a small

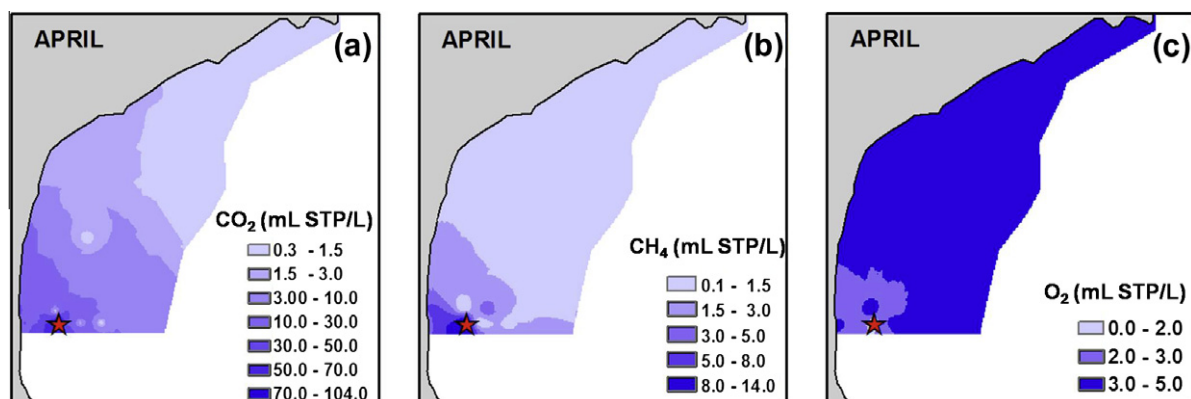


Fig. 5. (a–c) Distribution maps of the dissolved CO_2 , CH_4 and O_2 concentrations measured in the Levante Bay in April 2011.

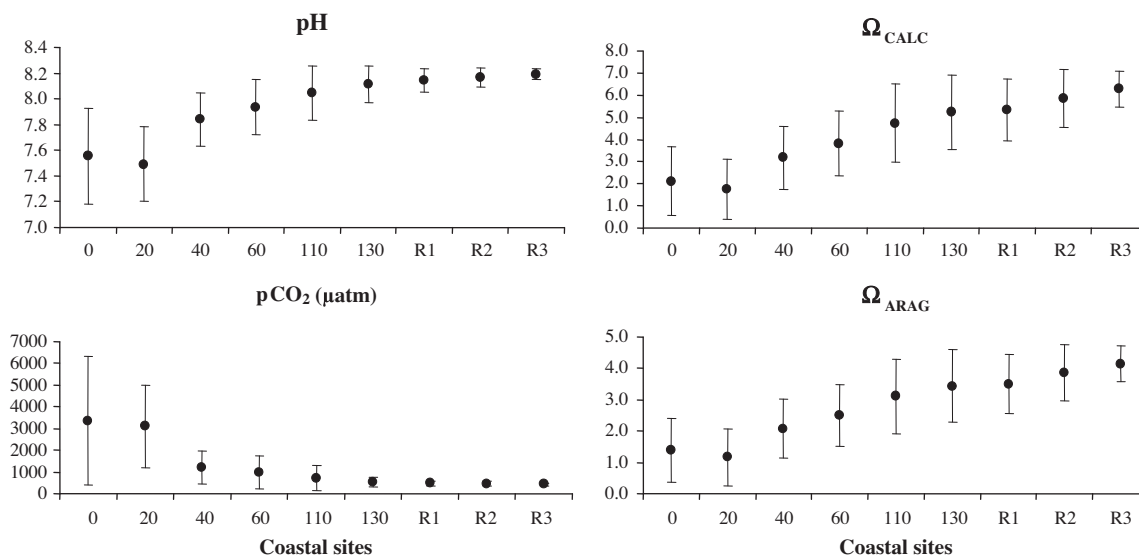


Fig. 6. Average (\pm S.D.) pH_T , pCO_2 , Ω_{CALC} and Ω_{ARAG} (September 2009–July 2011) at all nearshore sites positioned along the northern shore of Levante Bay ($n = 41$ for sites along the pH/pCO_2 gradient (0–130 sites); $n = 22$ for R1 and R2 sites; $n = 21$ for R3 site). See also Fig. 1 for location of sites.

Table 4
Average (\pm SD) seawater temperature, salinity and total alkalinity (TA) recorded from September 2009 to July 2011 at the northern transect of the Levante Bay, along the pH gradient (from site 0 to 130) and at the control sites (R1–R3).

	Temperature ($^{\circ}\text{C}$)	Salinity (‰)	n	TA ($\mu\text{mol kg}^{-1}$)	n (Missing data)
0	22.26 (± 4.96)	37.18 (± 1.34)	41	2541.3 (± 6.6)	9
20	21.70 (± 4.80)	37.39 (± 1.39)	41	2541.0 (± 2.8)	9
40	21.71 (± 4.95)	37.49 (± 0.63)	41	2524.7 (± 0.5)	9
60	21.67 (± 4.93)	37.59 (± 0.56)	41	2520.5 (± 6.5)	9
110	21.53 (± 4.82)	37.59 (± 0.62)	41	2526.6 (± 9.1)	9
130	21.63 (± 4.89)	37.63 (± 0.63)	41	2534.6 (± 26)	9
R1	21.66 (± 4.22)	37.45 (± 0.68)	22	2532.5 (± 21)	7 (November 2010; March 2011)
R2	22.66 (± 4.70)	37.44 (± 0.69)	22	2521.9 (± 6.5)	6 (November 2010; March & April 2011)
R3	23.96 (± 3.49)	37.35 (± 0.66)	19	2517.1 (± 4.4)	5 (November 2010; February–April 2011)

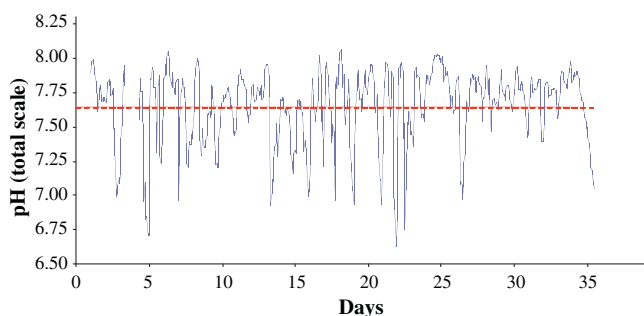


Fig. 7. Time series of hourly seawater pH values measured by a Honeywell Durafet pH sensor in a low pH site along the north shore (site 30, see Fig. 1). The time series was recorded from April 26th to May 30th, 2010. The dashed red line indicates the average pH value ($n = 807$).

proportion of the H_2S enters into the aquatic phase, where it oxidises to non-toxic sulphate due to the high O_2 saturation recorded in this part of the bay.

Careful selection of study areas around CO_2 vent systems provide opportunities to examine the ecological effects of pH variability to forecast organism responses to acidification in habitats exposed to large natural diel, semi-diurnal and stochastic fluctuations in the carbonate system (Kerrison et al., 2011).

The northern section of the shoreline had a variety of intertidal and subtidal communities including rocky substrata with algae,

sandy habitats, seagrass meadows and infralittoral boulder fields at <2 m depth. Early descriptions revealed that rich subtidal communities are present in this area. Whilst the Red Sea seagrass *Halophila stipulacea* (Rindi et al., 1999), benthic diatoms and cyanobacteria characterise the main CO_2 vents, perennial brown macroalgae (mostly *Sargassum* sp. and *Cystoseira* spp.) and *Cymodocea nodosa* beds are dominant along the northern shore of the Bay (Giaccone, 1969). Johnson et al. (2013) and Lidbury et al. (2012) found that increasing CO_2 concentrations significantly altered periphyton communities in Levante Bay; whilst Arnold et al. (2012) found that as CO_2 levels in the bay increases, the seagrass *C. nodosa* was less able to produce phenols which are important protective compounds from grazing, pathogens and UV rays.

Vulcano Island, like other volcanic sites in Southern Italy and Greece (Dando et al., 1999), shows how marine systems respond to long-term elevations in CO_2 such as those that could arise from geological sequestration leaks. As carbon capture and storage is being adopted as a CO_2 mitigation strategy, it is important to understand the associated risks such as leakage probability, strength of environmental perturbation, and any economic, and social impacts. Natural seabed CO_2 seeps clearly provide excellent opportunities for the development and testing of monitoring techniques for sub-seabed CO_2 leaks (Espa et al., 2010), and to assess the potential ecological impacts of marine CO_2 perturbations.

5. Conclusions

We show that even very large CO₂ seabed leakage has a relatively localised geochemical effect. Care is needed when using sites such as Levante Bay to predict effects of ocean acidification as parts of the bay contain low oxygen water, elevated levels of metals such as Fe and toxic compounds such as H₂S. The area close to the main vents is not well suited to studies of ocean acidification as it is subject to strong redox reactions, due to the input of reduced hydrothermal species (e.g. Fe²⁺ and H₂S) that dissolve in the oxidising sea-water. The area affected by these extreme conditions varies depending on wind driven water circulation within the bay. The northern part of the bay, in contrast, is well suited to studies of the effects of increased CO₂ levels where ecosystem processes such as production, competition and predation can be observed. In this part of the bay the saturation states of calcite and aragonite decrease gradually as CO₂ levels rise which is proving useful in studies of the localised effects of seabed carbon capture leakage and the chronic effects of ocean acidification.

Acknowledgements

We thank Mariagrazia Graziano and Roberto Sicari (University of Palermo) for their assistance with fieldwork in Vulcano Island and Lorenzo Brusca and Sergio Bellomo (INGV, Palermo) for laboratory analyses. This work was funded by the EU 'Mediterranean Sea Acidification under a changing climate' project (MedSea; grant agreement 265103).

References

- Aiuppa, A., Dongarrà, G., Capasso, G., Allard, P., 2000. Trace elements in the thermal groundwaters of Vulcano Island (Sicily). *J. Volcanol. Geoth. Res.* 98, 189–207.
- Amend, J.P., Rogers, K.L., Shock, E.L., Inguaggiato, S., Gurrieri, S., 2003. Energetics of hemolithoautotrophy in the hydrothermal system of Vulcano Island, southern Italy. *Geobiology* 1, 37–58.
- Arnold, T., Mealey, C., Leahy, H., Miller, A.W., Hall-Spencer, J.M., Milazzo, M., Maers, K., 2012. Ocean acidification and the loss of protective phenolics in seagrasses. *PLoS One* 7 (4), e35107.
- Barberi, F., Innocenti, F., Ferrara, G., Keller, J., Villari, L., 1974. Evolution of the Aeolian arc volcanism (Southern Tyrrhenian sea). *Earth Planet Sci. Lett.* 21, 269–276.
- Beccaluva, L., Gabbianelli, G., Lucchini, R., Rossi, P.L., Savelli, C., 1985. Petrology and K/Ar ages of volcanic dredged from the Aeolian seamounts: implications for geodynamic evolution of the southern Tyrrhenian basin. *Earth Planet Sci. Lett.* 74, 187–208.
- Caldeira, K., Wickett, M.E., 2003. Anthropogenic carbon and ocean pH. *Nature* 425, 365.
- Capaccioni, B., Tassi, F., Vaselli, O., 2001. Organic and inorganic geochemistry of low temperature gas discharges at the Baia di Levante beach, Vulcano Island, Italy. *J. Volcanol. Geoth. Res.* 108, 173–185.
- Carapezza, M.L., Barberi, F., Ranaldi, M., Ricci, T., Tarchini, L., Barrancos, J., Fisher, C., Perez, N., Weber, K., Di Piazza, A., Gattuso, A., 2011. Diffuse CO₂ soil degassing and CO₂ and H₂S concentrations in air and related hazards at Vulcano Island (Aeolian arc, Italy). *J. Volcanol. Geoth. Res.* 204, 130–144.
- Chiodini, G., Cioni, R., Marini, L., 1993. Reactions governing the chemistry of crater fumaroles from Vulcano Island, Italy, and implications for volcanic surveillance. *Appl. Geochem.* 8, 357–371.
- Chiodini, G., Cioni, R., Marini, L., Panichi, C., 1995. Origin of the fumarolic fluids of Vulcano Island, Italy and implications for volcanic surveillance. *Progr. Oceanogr.* 57, 99–110.
- Dando, P.R., Stüben, D., Varnavas, S.P., 1999. Hydrothermalism in the Mediterranean Sea. *Progr. Oceanogr.* 44, 333–367.
- DOE, 1994. Handbook of methods for the analysis of the various parameters of the carbon dioxide system in sea water. Version 2. ORNL/CDIAC-74. In: Dickson, A.G., Goyet, C. (Eds.), Carbon Dioxide Information Analysis Center. Oak Ridge National Laboratory, US Department of Energy, Oak Ridge, Tennessee.
- Drever, J.I., 1997. The Geochemistry of Natural Waters: Surface and Groundwater Environments, third ed. Prentice Hall, Upper Saddle River, N.J.
- Espa, S., Caramanna, G., Bouche, V., 2010. Field study and laboratory experiments of bubble plumes in shallow seas as analogues of sub-seabed CO₂ leakages. *Appl. Geochem.* 25, 696–704.
- Fabricius, K.E., Langdon, C., Uthicke, S., Humphrey, S., Noonan, S., Dèath, G., Okazaki, R., Muehllehner, N., Glas, M.S., Lough, J.M., 2011. Losers and winners in coral reefs acclimatized to elevated carbon dioxide concentrations. *Nature Clim. Change* 1, 165–169.
- Frazzetta, G., La Volpe, L., Sheridan, M.F., 1984. Evolution of the Fossa cone, Vulcano. *J. Volcanol. Geoth. Res.* 17, 139–360.
- Giaccone, G., 1969. Associazioni algali e fenomeni secondari di vulcanismo nelle acque marine di Vulcano (Mar Tirreno). *Giorn. Bot. Ital.* 103, 353–366.
- Hall-Spencer, J.M., Rodolfo-Metalpa, R., Martin, S., Ransome, E., Fine, M., Turner, S.M., Rowley, S.J., Tedesco, D., Buia, M., 2008. Volcanic carbon dioxide vents show ecosystem effects of ocean acidification. *Nature* 454, 96–99.
- Hofmann, G.E., Smith, J.E., Johnson, K.S., Send, U., Levin, L.A., Micheli, F., Paytan, A., Price, N.N., Peterson, B., Takeshita, Y., Matson, P.G., Crook, E.D., Kroeker, K.J., Gambi, M.C., Rivest, E.B., Frieder, C.A., Yu, P.C., Martz, T.R., 2011. High-frequency dynamics of ocean pH: a multi-ecosystem comparison. *PLoS One* 6 (12), e28983, Epub 2011 Dec 19.
- Inguaggiato, S., Mazot, A., Diliberto, I.S., Inguaggiato, C., Madonia, P., Rouwet, D., Vita, F., 2012. Total CO₂ output from Vulcano Island (Aeolian Islands, Italy). *Geochem. Geophys. Geosyst.* 13, Q02012. <http://dx.doi.org/10.1029/2011GC003920>.
- Italiano, F., Nuccio, P.M., Sommaruga, C., 1984. Gas/steam and thermal energy release measured at the gaseous emissions of the Baia di Levante of Vulcano Island, Italy. *Acta Vulcanologica* 5, 89–94.
- Italiano, F., 2009. Hydrothermal fluids vented at shallow depths at the Aeolian islands: relationships with volcanic and geothermal systems. *FOG - Freiberg Online Geology*, 22, 55–60.
- Johnson, V.R., Brownlee, C., Rickaby, R.E.M., Graziano, M., Milazzo, M., Hall-Spencer, J.M., 2013. Responses of marine benthic microalgae to elevated CO₂. *Mar. Biol.* <http://dx.doi.org/10.1007/s00227-011-1840-2>.
- Kadar, E., Fisher, A., Stolpe, B., Harrison, R.M., Parello, F., Lead, J., 2012. Metallic nanoparticle enrichment at low temperature, shallow CO₂ seeps in Southern Italy. *Mar. Chem.* 140–141, 24–32.
- Keller, J., 1980. The Island of Vulcano. In: Villari, L. (Ed.), *The Aeolian Islands, an Active Volcanic Arc in the Mediterranean Sea*. Società Italiana di Mineralogia e Petrologia, Milano, pp. 29–74.
- Kerrison, P., Hall-Spencer, J.M., Suggett, D.J., Hepburn, L.J., Steinke, M., 2011. Assessment of pH variability at a coastal CO₂ vent for ocean acidification studies. *Estuar. Coast Shelf S.* 94, 129–137.
- Lidbury, I., Johnson, V., Hall-Spencer, J.M., Munn, C.B., Cunliffe, M., 2012. Community-level response of coastal microbial biofilms to ocean acidification in a natural carbon dioxide vent ecosystem. *Mar. Poll. Bull.* 64, 1063–1066.
- Liotta, M., Martelli, M., 2012. Dissolved gases in brackish thermal waters: an improved analytical method. *Geofluids* 12, 236–244. <http://dx.doi.org/10.1111/j.1468-8123.2012.00365.x>.
- Middelboe, A.L., Hansen, P.J., 2007. Direct effects of pH and inorganic carbon on macroalgal photosynthesis and growth. *Mar. Biol.* 151, 134–144.
- Mikaloff-Fletcher, S.E., Gruber, N., Jacobson, A.R., Doney, S.C., Dutkiewicz, S., Gerber, M., Follows, M., Joos, F., Lindsay, K., Menemenlis, D., Mouchet, A., Mueller, S.A., Sarmiento, J.L., 2006. Inverse estimates of anthropogenic CO₂ uptake, transport, and storage by the ocean. *Global Biogeochem. Cy.* 20, GB2002.
- Millero, F.J., Schreiber, D.R., 1982. Use of the ion-pairing model to estimate activity-coefficients of the ionic components of natural-waters. *Am. J. Sci.* 282, 1508–1540.
- Pierrot, D., Lewis, E., Wallace, D.W.R., 2006. MS Excel Program Developed for CO₂ System Calculations. ORNL/CDIAC-105a. Carbon Dioxide Information Analysis Center, Oak Ridge National Laboratory, US Department of Energy, Oak Ridge, Tennessee.
- Riebesell, U., Schulz, K.G., Bellerby, R.G.J., Botros, M., Fritsche, P., Meyerhöfer, M., Neill, C., Nondal, G., Oeschles, A., Wohlers, J., Zöllner, E., 2007. Enhanced biological carbon consumption in a high CO₂ ocean. *Nature* 450, 545–548.
- Rindi, F., Maltagliati, F., Rossi, F., Acunto, S., Cinelli, F., 1999. Algal flora associated with a *Halophila stipulacea* (Forsskål) Ascherson (Hydrocharitaceae, Helobiae) stand in the western Mediterranean. *Oceanologica Acta* 22, 421–429.
- Roberts, D.A., Birchenough, S.N.R., Lewis, C., Sanders, M.B., Bolam, T., Sheahan, D., 2013. Ocean acidification increases the toxicity of contaminated sediments. *Glob. Change Biol.* <http://dx.doi.org/10.1111/gcb.12048>.
- Rogers, K.L., Amend, J.P., Gurrieri, S., 2007. Temporal changes in fluid chemistry and energy profiles in the Vulcano Island hydrothermal system. *Astrobiology* 7, 905–932. <http://dx.doi.org/10.1089/ast.2007.0128>.
- Roy, R.N., Roy, L.N., Vogel, K.M., Porter-Moore, C., Pearson, T., Good, C.E., Millero, F.J., Campbell, D.M., 1993. The dissociation constants of carbonic acid in seawater at salinities 5–45 and temperatures 0–45 °C. *Mar. Chem.* 44, 249–267.
- Sabine, C.L., Feely, R.A., Gruber, N., Key, R.M., Lee, K., Bullister, J.L., Wanninkhof, R., Wong, C.S., Wallace, D.W.R., Tilbrook, B., Millero, F.J., Peng, T., Kozyr, A., Ono, T., Rios, A.F., 2004. The oceanic sink for anthropogenic CO₂. *Science* 305, 367–371.
- Sedwick, S., Stüben, D., 1996. Chemistry of shallow submarine warm springs in an arc-volcanic setting: Vulcano Island, Aeolian Archipelago, Italy. *Mar. Chem.* 53, 147–161.
- Sicardi, L., 1940. Il recente ciclo dell'attività fumarolica dell'isola di Vulcano. *Boll. Volcanol.* 7, 85–139.
- Silvestri, O., Mercalli, G., 1891. Modo di presentarsi e cronologia delle esplosioni eruttive di Vulcano cominciate il 3–8-1888. *Ann. R. Uff. Cent. Meteor. Geodin.* 4, 120–190.
- Solomon, S., Qin, D., Manning, M., Chen, Z., Marquis, M., Averyt, K.B., Averyt, Tignor, M., Miller, H.L., 2007. Contribution of Working Group I to the Fourth Assessment Report of the Intergovernmental Panel on Climate Change. Cambridge, U.K., New York, USA.
- Sommaruga, C., 1984. Le ricerche geotermiche svolte a Vulcano negli anni '50. *Rendiconti della Soc. It. Mineral. Petrol.* 39, 355–366.

Tedesco, D., Miele, G., Sano, Y., Toutain, J.P., 1995. Helium isotopic ratio in Vulcano island fumaroles: temporal variations in shallow level mixing and deep magmatic supply. *J. Volcanol. Geoth. Res.* 64, 117–128.

Turekian, K.K., 1968. *Oceans*. Prentice-Hall, Englewood Cliffs, New Jersey, USA, 149 pp.

United Nations, 2001. Department of Economic and Social Affairs New York, Population Division, DRAFT ESA/P/WP.165.

Wilson, T.R.S., 1975. The major constituents of seawater. In: Riley, J.P., Skirrow, G. (Eds.), *Chemical Oceanography*, second ed. Academic Press, pp. 365–413 (1).